Microsc. Microanal. Microstruct. **4** (1993) 287–296 APRIL/JUNE **1993**, PAGE 287

Classification
Physics Abstracts
61.16D — 64.70 — 68.40

In-situ observation and the thermodynamical analysis of the melting process of In particles embedded in an Al matrix

K. Sasaki and H. Saka

Faculty of Engineering, Nagoya University, Furo-cho, Chikusa-ku, Nagoya, 464-01, Japan

(Received February 8, 1993; accepted March 26, 1993)

1. Introduction.

Crystalline solid-liquid and solid-solid interfaces play an important role in controlling properties of materials [1]. Between the dimensions on an atomic scale and the dimensions which characterize bulk material is to be found a size range where the surfaces and interfaces control the phase transformation of materials. The melting of microcrystals at temperatures below the bulk melting temperature was first demonstrated by Takagi [2]. The experimental and theoretical works after the Takagi's work have pointed out an important role of the properties of the surface and interface [3-5] in the melting phenomenon of microcrystals. In order to reveal the role of the interfaces during the melting process on In particles embedded in an Al matrix, an *in-situ* heating experiment in a high resolution/high voltage electron microscope was performed [6].

2. Experimental procedures.

The Al-In system has a monotectic system [7]. The mutual solubility between In and Al is very small below 300 °C. Thus, the processes of the melting and freezing of 'pure' In dispersed in an Al matrix could be observed. An Al-4.5at%In alloy was prepared by splat-quenching from nominally pure (99.999%) starting materials of Al and In [8]. TEM specimens were prepared by standard electro-polishing.

The TEM observation was performed in Hitachi H-1250ST operating at 1000 kV. The specimen was observed on a double tilting and heating holder. The temperature of the specimen in the electron microscope was kept just below the melting point of In until the drift of the specimen became negligibly small. Then, additional heating was introduced by focusing the electron beam in a small selected area, leading to the melting of the In particles in that region. Lattice fringes of In and Al were observed in the whole process of melting as shown in figure 1. The disappearance of moire' fringe between In and Al matrix following the melting of In (Fig. 1) was used to identify the region of the molten In.

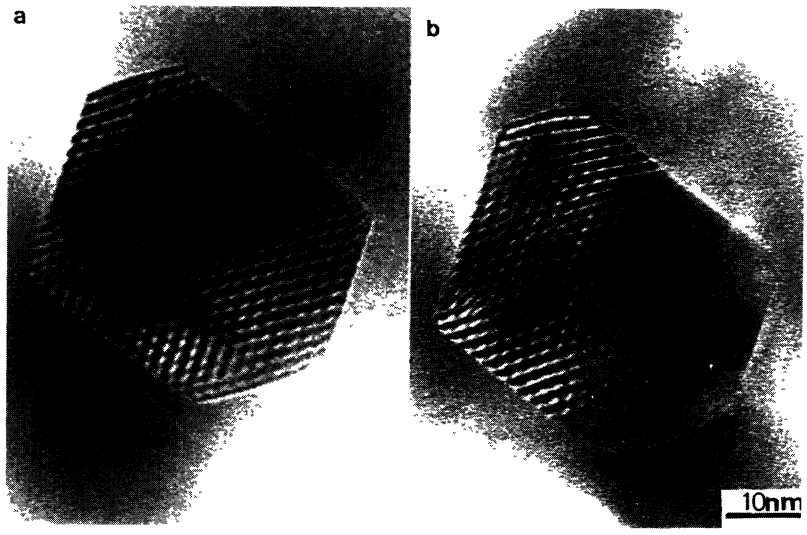

Fig. 1. — High resolution images of the melting process of an In particle viewed along the <110> direction. Moire' fringes which are observed in the whole area (a) and in the left hand side of the In particle (b) indicate the area of solid In.

3. Results.

The In particles were cuboctahedral in shape bounded by eight $\{111\}_{Al,\ In}$ and six $\{100\}_{Al,\ In}$ facets as shown schematically in figure 2. In many cases, one void was observed on one of the $\{100\}_{Al,\ In}$ facets of each particle. During the heating experiment, the sample was heated and cooled at a heating and cooling rate in the range $1 \sim 2$ K/hr around the melting temperature of In particles. After the heating experiment for about 10^5 seconds, there was no change in either the In particle shape or the orientation relationship between the In particles and the Al matrix [6, 9]. The melting process of In particles proceeds in six stages, at each of which one of the {100} facets becomes covered successively with the liquid phase as illustrated in figure 2. Initially, the liquid droplet is nucleated at a {100} facet or at the cavity which is in contact with one of the {100} facets (Fig. 2a), and repeatedly expands and shrinks as shown in figure 3 (Stage 1). The liquid droplet shows the most shrinkage in the shape viewed along a <110> and <100> direction in figures 3a and 3c, respectively. The most expansion of the liquid droplet viewed along the <110> direction is shown in figure 3b. The interface between solid and liquid In (In_s/In_l) showed a flip-flop like motion between two shapes. The time spent in this stage was longest in the whole process of melting. Stage 2 (Fig. 2b): the hemispherical In_s/In_l interface started to propagate into the interior of the In particle, and reached one of the four nearest {100} facets as shown in figure 4a. Stage 3 (Fig. 2c): the liquid phase expanded further and covered the other of the nearest {100} facets. Stage 4 (Fig. 2d): the In_s/In_l interface was anchored at the two vertices at each of which two {111} facets and a {100} facet come together and bowed out (Fig. 4b). Stage 5 (Fig. 2e): one of the last two {100} facets which had not been covered with the liquid phase now became covered with the liquid phase, and the In_s/In_l interface became parallel to the {100} facet (Fig. 4c). Stage 6 (Fig. 2f): the In_s/In_l interface propagated, while keeping the interface parallel to the {100} plane, until the whole volume of the In particle melted. These melting processes were observed in the particles whose {100} facet separations are larger than 100 Å. These intermediate stages of melt-

ing in the particle smaller than 100 Å have not been observed. The difference of the melting process between particles larger than 100 Å and those smaller than 100 Å is also suggested by the relation between superheating temperature (ΔT) and reciprocal length of the {100} facet separation ($1/L$) [8] as shown in figure 5. Δ Ts of the particles smaller than 100 Å are on the straight line through the original point with a slop $\Delta\, TL = 2000$ Å K. The straight line, however, could not be drawn for the Δ Ts of the particles larger then 100 Å.

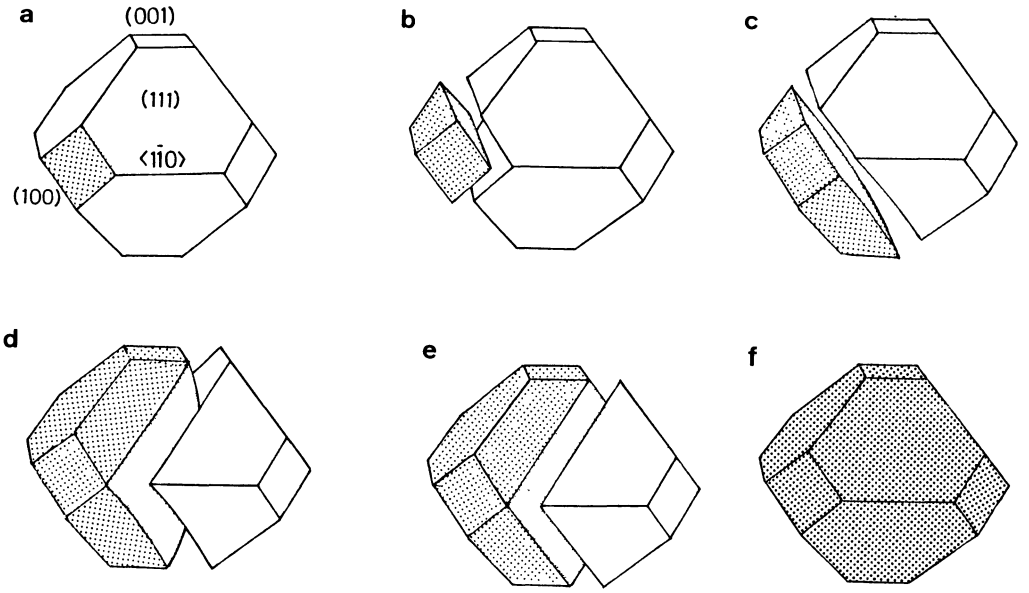

Fig. 2. — Schematic diagrams of the melting process of the In particle embedded in an Al matrix. Hatching indicates the liquid of In.

4. Discussion.

The relation among the interfacial energy per unit area of the interfaces concerning the melting process could be determined as the result of the detailed observation of the process. The relationship between the interfacial energy per unit area of the interface between soldi Al an In on the {100} (σ_1) and the {111} (σ_2) facet can be written as $h_{100}/\sigma_1 = h_{111}/\sigma_2$ using by Curie-Wulff theorem. Where h_{100} and h_{111} are the one half of the {100} and {111} facet separation, respectively. Substituting the value of $k \equiv h_{100}/h_{111}$ measured from figure 1a, we obtain $\sigma_1 = 1.20$ ($\pm$ 0.06) σ_2. The interface between solid Al and liquid In parallel to {111} persists after the In particle becomes molten completely. That means that the interfacial energy per unit area on this plane (σ_3) is much lower than that on the plane with other orientations (σ_4). The relative values of the interfacial energies per unit area σ_1, σ_2, σ_3, σ_4 and those of the In_s/In_l interface (σ_5) were determined from the contact angles between interfaces during the melting process as follows.

In stage 1, a droplet of liquid In is nucleated on a {100} solid Al/In interface. As illustrated in

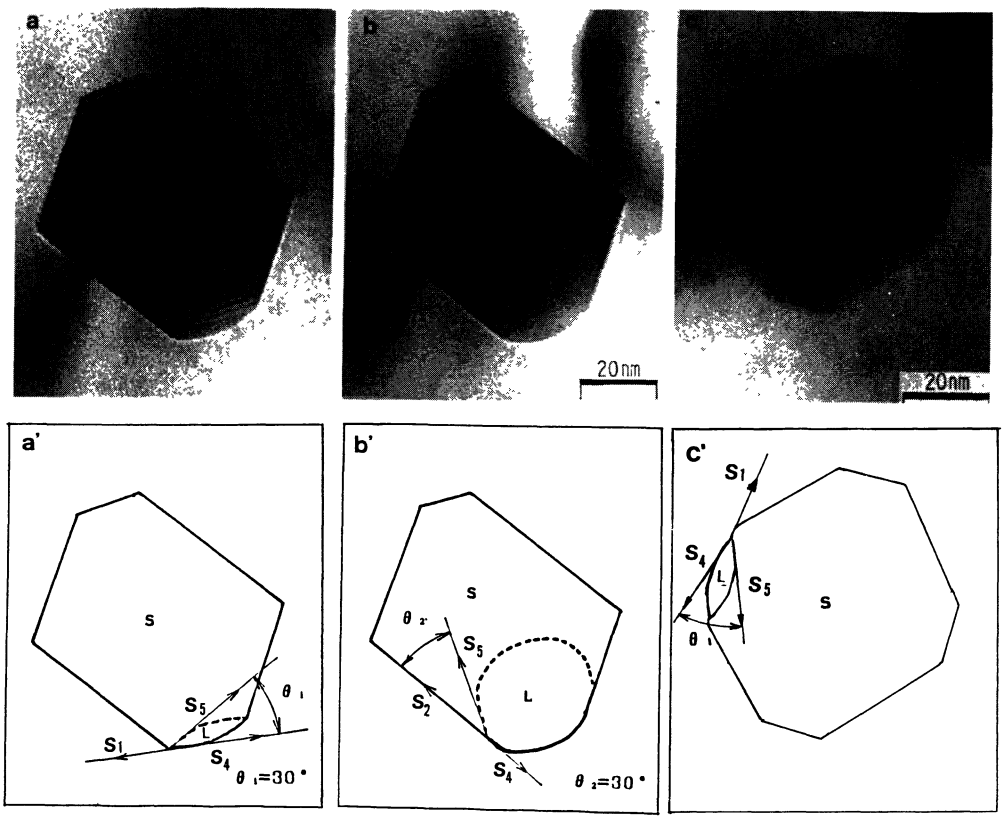

Fig. 3. — TEM micrographs of the melting process of an In particle viewed along [011] (a,b) and [001] (c) and schematic diagrams (a',b') and (c') corresponding to (a,b) and (c), respectively. The areas indicated by S and L correspond to solid and liquid In, respectively.

figure 3a', the relation among σ_1, σ_4 and σ_5 can be written by

$$\sigma_4 + \sigma_5 \cos\theta_1 = \sigma_1 \tag{1}$$

where θ_1 is the contact angle between the In_s/In_l interface and the interface between solid Al and liquid In, which is measured from figure 3a to be 30° ± 10°. This relation is more apparent in figure 3c. The droplet is not expanding fully on the {100} facet, so that we can observe that the interface between solid Al and In on the {100} plane is in a balance against the In_s/In_l interface and the interface between solid Al and liquid In as illustrated in figure 3c. The geometrical relation between figures 3a and 3c is illustrated in figure 6 schematically. At the largest bowing out of the In droplet in stage 1, as illustrated in figure 3b, the relation among σ_2, σ_4 and σ_5 can be written by

$$\sigma_4 = \sigma_2 + \sigma_5 \cos\theta_2 \tag{2}$$

where θ_2 is the contact angle between the In_s/In_l interface and the interface between solid Al and In on the {111} plane, which is measured from figure 3b to be 30° ± 10°. In stage 4, as illustrated in figure 4c', the relation among σ_3, σ_2 and σ_5 can be written by

$$\sigma_3 = \sigma_2 + \sigma_5 \cos\theta_3 \tag{3}$$

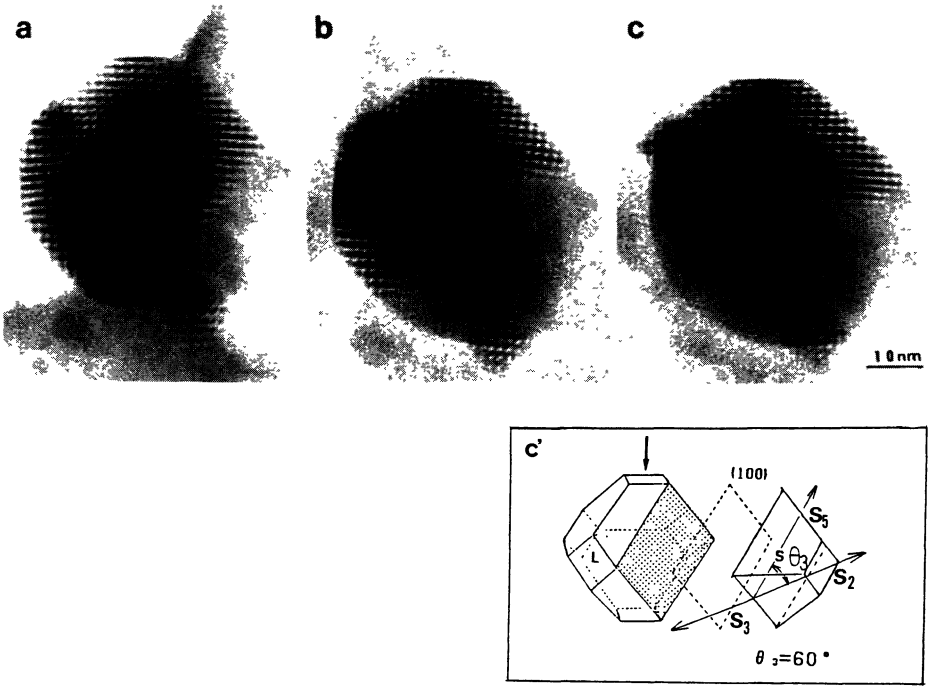

Fig. 4. — TEM micrographs of the melting process of an In particle viewed along [001] (a,b,c) and a schematic diagram (c') corresponding to (c). The areas indicated by S and L correspond to solid and liquid In, respectively.

where θ_3 is the contact angle between the In_s/In_l interface and the interface between solid Al and liquid In on {111}, which is measured from figure 4c to be $60° \pm 10°$. Equations (1, 2) and (3) give the following relation among σ_1, σ_2, σ_3, σ_4 and σ_5.

$$\sigma_1 = 1.20(\pm 0.06)\sigma_2 > \sigma_4 = 1.105(\pm 0.038)\sigma_2 > \sigma_3 = 1.067(\pm 0.042)\sigma_2 > \sigma_2 > \sigma_5 = 0.122(\pm 0.048)\sigma_2 \quad (4)$$

Allen, Gile and Jesser [10] analyzed the superheating temperature ΔT of particles embedded in a matrix by thermodynamic theory [4]. They describe the relation between the ΔT and the radius of the particle (r) using the model of spherical shape particles as follows

$$\Delta T = (T_m/\Delta H)\{3(\sigma_s - \sigma_L)/r - \Delta E\} \quad (5)$$

where T_m is the melting temperature of bulk In, ΔH the latent heat, ΔE the change in strain energy density on melting, σ_s and σ_L the interfacial energy per unit area between the particle and matrix before and after melting, respectively. According to equation (5), the relation between ΔT and $1/r$ will draw a straight line. That is corresponding to the region of the particles smaller than 100 Å as shown in figure 5. Now we know not only the detailed shape on the In particle but also the relation among the interfaces concerning the melting process. This means that the assumption of the spherical shape of the particle is not required and the detail of σ_s, σ_L can be written. The interfacial energy between solid Al and In $(4\pi r^2 \sigma_s)$ can be written by

$$4\pi r^2 \sigma_s = A_1 \sigma_1 + A_2 \sigma_2 \quad (6)$$

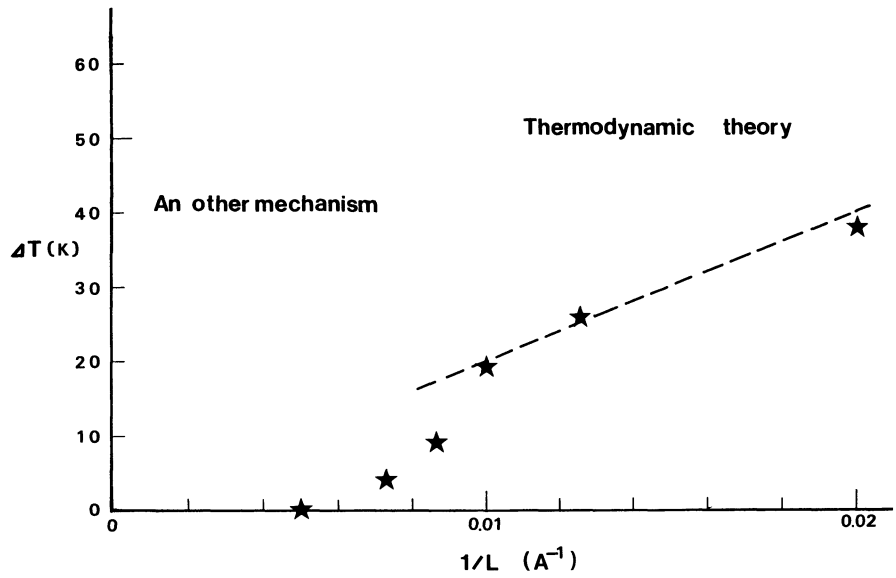

Fig. 5. — The relation between superheating temperature (ΔT) and reciprocal length of the {100} facet separation ($1/L$) [8]. The ΔTs of the particle smaller than 100 Å are on the straight line through the original point with a slop $\Delta TL = 2000$ Å K.

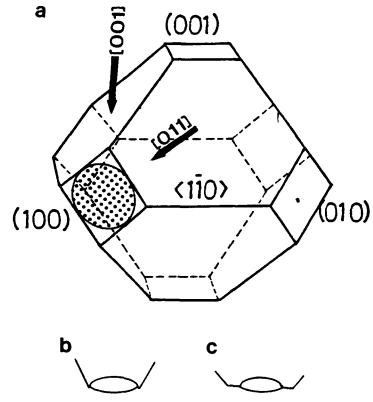

Fig. 6. — Schematic illustration of the relation between the shape of the liquid droplet (hatching in (a)) of In on the (100) facet viewed along [011] (Fig. 3a) and [001] (Fig. 3c). Although the droplet does not expand full of the (100) facet (a), the [011] projection (b) shows that the (100) facet is covered by liquid In, completely. The solid Al and In interface which surrounds the liquid droplet on the (100) facet can be observed in the [001] projection (c).

where A_1 and A_2 are the area of the interface between solid Al and In on {100} and {111}, respectively. These two areas A_1 and A_2 can be calculated as a simple geometrical problem of cuboctahedron. The specific lengths from l_0 to l_6 of cuboctahedral In particle, which will help the calculation of A_1 and A_2, are shown in figure 7a. All these lengths can be described using by the {100} facet separation $L\,(= 2h_{100})$ and the ratio between the {100} and {100} facet separation

$k\,(= h_{100}/h_{111})$. The geometrical representation of the calculation of A_1 and A_2 are illustrated in figures 7b and 7c, respectively. A_1 and A_2 can be written by

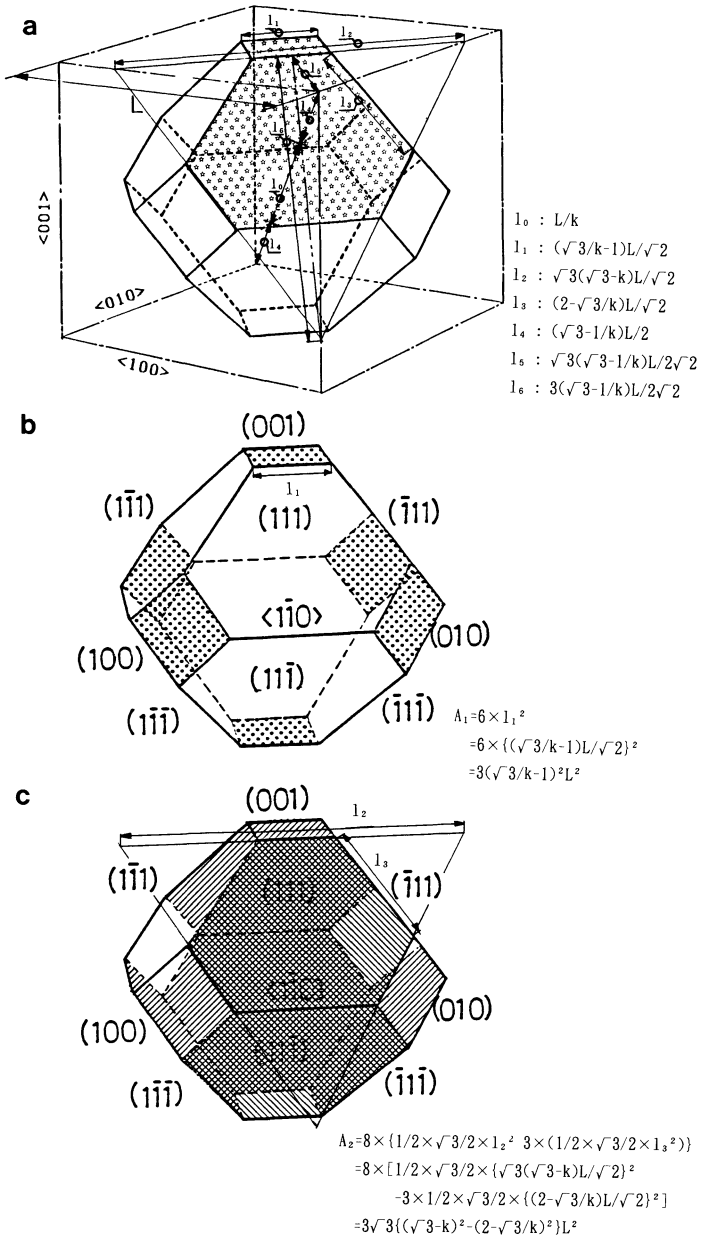

Fig. 7. — Schematic representation of the geometrical property of cuboctahedron. The lengths from l_0 to l_6 can be described by L and k (a). The area of A_1 is six times of the area of a $\{100\}$ facet, which can be written by l_1^2 (b). The area of A_2 is eight times of the area of a $\{111\}$ facet, which can be written by $1/2 \times \sqrt{3}/2 \times l_2^2 - 3\times \left(1/2 \times \sqrt{3}/2 \times l_3^2\right)$ (c).

$$A_1 = 6l_1^2 = 3(\sqrt{3}/k - 1)^2 L^2 \tag{7a}$$

$$A_2 = 8 \times \{1/2 \times \sqrt{3}/2 \times l_2^2 - 3 \times (1/2 \times \sqrt{3}/2 \times l_3^2)\}$$
$$= 3\sqrt{3}\{(\sqrt{3} - k)^2 - (2 - \sqrt{3}/k)^2\} L^2 \tag{7b}$$

The interfacial energy between solid Al and liquid In $(4\pi r^2 \sigma_L)$ can be written by

$$4\pi r^2 \sigma_L = A_3 \sigma_3 + A_4 \sigma_4 \tag{8}$$

where A_3 and A_4 are the area of the interface between solid Al and liquid In on {111} and other plane, respectively. The area of A_3 and A_4 are approximately equal to A_2 and A_1, respectively. The volume of a particle V_0 can be written by

$$V_0 = \{1 - \sqrt{3}/2(\sqrt{3} - k)^3 + (2 - \sqrt{3}/k)^3/2\} L^3 \tag{9}$$

If we put

$$a_1 \equiv 3(\sqrt{3}/k - 1)^2, \quad a_2 \equiv 3\sqrt{3}\{(\sqrt{3} - k)^2 - (2 - \sqrt{3}/k)^2\}$$
$$v_0 \equiv \{1 - \sqrt{3}/2(\sqrt{3} - k)^3 + (2 - \sqrt{3}/k)^3/2\} \tag{10}$$

Equation (5) can be rewritten using by equations (6,7,8,9) and (10) as follow

$$\Delta T = -(T_m/\Delta H)\{(\sigma_1 a_1 + \sigma_2 a_2) - (\sigma_3 a_2 + \sigma_4 a_1)\}/v_0 L - \Delta E \tag{11}$$

The corresponding value of L in spherical model is the diameter $2r(= 0.91L)$ of the particle. In the region of the L is less than 100 Å where the thermodynamic theory [4] is controlling the melting of the particle, we can put the value of $\Delta TL = 2000$ Å K into equation (11). The value of the bulk In of ΔH was used for the calculation. As the result of the substitution of equation (4) into equation (11), the absolute values of the interfacial energy per unit area σ_1, σ_2, σ_3, σ_4 and σ_5 were determined as follows

$$\sigma_1 = 257 \pm 115 \ \left(\text{erg/cm}^2\right)$$
$$\sigma_2 = 242 \pm 121 \ \left(\text{erg/cm}^2\right)$$
$$\sigma_3 = 253 \pm 124 \ \left(\text{erg/cm}^2\right)$$
$$\sigma_4 = 231 \pm 99 \ \left(\text{erg/cm}^2\right)$$
$$\sigma_5 = 31 \pm 20 \ \left(\text{erg/cm}^2\right)$$

The interfacial energy per unit area of the interface between solid Al and liquid In determined by dihedral angle method [11] to be 322 ± 24 erg/cm^2, which can be calculated by equation (14) in reference is in good agreement with the value of σ_3 and σ_4. The interfacial energy per unit area on In_s/In_l interface σ_5 also shows good agreement with the value determined by Allen *et al.* [12].

These agreements mean the following results.

1) That is a proof of that the thermodynamic theory [4] is controlling the melting process of the particle smaller than 100 Å.

2) The value of bulk material of ΔH can be applied to the calculation means that the difference of the pressure due to the volume change on melting which will cause the change of latent heat ΔH and also strain energy density ΔE on melting is negligible. That is presumably due to the presence of the void contacting the particle. The formation of the void can be understood when we take into account the process of solidification of this material. In the Al-In phase diagram [7], Al solidifies at 912 K and In rich liquid is left in the Al matrix at the composition of our sample. The In rich liquid will deposit Al onto the interface between solid Al and the liquid between 912 K and 450 K. At the melting point of In, pure In liquid will be left in the Al matrix. The volume change $(V_s - V_l)/V_l = -2.6\%$ on solidification of In causes the void which is in contact with the In particle. That void would have enough volume to cancel the volume change on melting of the In particle.

3) The step by step propagation of the melting of In into the particle (six stages of melting process) lowers the superheating temperature of the particle larger than 100 Å.

5. Conclusions.

The melting process of In particles embedded in an Al matrix, which was prepared by splat quenching, has been observed, continuously. The interfacial energies of solid-liquid interface of In, the interfaces between solid Al and In, and solid Al and liquid In were thermodynamically analyzed, and the following results have been obtained.

1) In the region of the particle larger than 100 Å, melting started either at a cavity or at one of the {100} facets and proceeded into the interior of the In particle in six stages in such a way that, at each of the stages, one of the {100} facets became covered with the liquid phase. These processes lower the superheating temperature of the particles compared to the particles smaller than 100 Å.

2) In the region of the particle smaller than 100 Å, these intermediate stages of the melting have not been observed and the relation between superheating temperature and the particle diameter obeys the thermodynamic theory [4].

3) The absolute values of interfacial energy per unit area for all interfaces concerning the melting process were determined.

4) The effect of volume change on melting process is negligible in the case of the In particles embedded in an Al matrix.

Acknowledgements.

This work was supported by the Grant-in-Aid for Encouragement of Young Scientists No.04750604 from Ministry of Education on Science and Culture and the Kazato Research Foundation.

References

[1] MOORE K., CHATTOPADHYAY K. and CANTOR B., *Proc. R. Soc. Lond.* **A414** (1987) p. 499.
[2] TAKAGI M., *J. Phys. Soc. Jpn.* **9** (1954) p. 359.
[3] BERMAN R. and CURZON A., *Canadian J. Phys.* **52** (1974) p. 923.
[4] COUCHMAN P. and JESSER, *Nature* **269** (1977) p. 481.
[5] SKRIPOV V., KOVERDA V. and SKOKOV V., *Phys. Stat. Sol.* **A66** (1981) p. 109.
[6] SASAKI K. and SAKA H., *Phil. Mag.* **A63** (1991) p. 1207.

[7] "Binary Alloy Phase Diagrams", Eds. T. Massalski, J. Murray, L. Bennett and H. Baker, *Am. Soc. Metals* (Metals Park, 1986).
[8] SAKA H., NISHIKAWA Y. and IMURA T., *Phil. Mag.* **A57** (1988) p. 895.
[9] ZHANG D. and CANTON B., *Phil. Mag.* **A62** (1990) p. 557.
[10] ALLEN G., GILE W. and JESSER W., *Acta Metall.* **28** (1980) p. 1695.
[11] CAMEL D., EUSTATHOPOULOS N.E. and DESRE P., *Acta Metall.* **28** (1980) p. 239.
[12] ALLEN G., BAYLES R., GILE W. and JESSER W., *Thin Solid Films* **144** (1986) p. 297.